Multi-parameter Vulnerability Analysis of Settlement-Affected Masonry Buildings with Shallow/Piled Foundations

Case Studies in The Netherlands

Nicodemo, G.; Peduto, D.; Korff, M.; Ferlisi, S.

DOI
10.1007/978-3-030-21359-6_5

Publication date
2020

Document Version
Final published version

Published in
CNRIG 2019: Geotechnical Research for Land Protection and Development

Citation (APA)
Nicodemo, G., Peduto, D., Korff, M., & Ferlisi, S. (2020). Multi-parameter Vulnerability Analysis of Settlement-Affected Masonry Buildings with Shallow/Piled Foundations: Case Studies in The Netherlands. In *CNRIG 2019: Geotechnical Research for Land Protection and Development* (pp. 42-51). (Lecture Notes in Civil Engineering; Vol. 40). Springer. https://doi.org/10.1007/978-3-030-21359-6_5

Multi-parameter Vulnerability Analysis of Settlement-Affected Masonry Buildings with Shallow/Piled Foundations: Case Studies in The Netherlands

G. Nicodemo[1(✉)], D. Peduto[1], M. Korff[2,3], and S. Ferlisi[1]

[1] Department of Civil Engineering, University of Salerno, Via Giovanni Paolo II, 132, 84084 Fisciano (SA), Italy
gnicodemo@unisa.it
[2] Deltares, P.O BOX, 177, 2600 MH Delft, The Netherlands
[3] Faculty of Civil Engineering and Geosciences, Delft University of Technology, Stevinweg 1, 2628 CN Delft, The Netherlands

Abstract. The paper presents a probabilistic analysis aimed at identifying the most appropriate subsidence related intensity (SRI) parameter (e.g., differential settlement, relative rotation, deflection ratio) that can be used to forecast the severity level of building damage at municipal scale through the generation of empirical fragility and vulnerability curves. The analysis refers to a rich sample of more than seven hundred monitored (by remote sensing techniques) and surveyed masonry buildings – mainly resting with their (shallow or piled) foundations on highly compressible fine-grained "soft soils" – affected by settlements in four urban areas in The Netherlands. The achieved outcomes, once further calibrated and validated, could allow for an improvement of existing geotechnical damage criteria for buildings as well as help local authorities in charge of the management/protection of subsiding urban areas to plan adequate foundation repairing/replacing measures before damage reaches intolerable severity levels.

Keywords: Soft soils · Settlements · Masonry buildings · Vulnerability

1 Introduction

The analysis and prediction of the vulnerability of buildings resting with their foundation systems on highly compressible fine-grained "soft soils" containing (organic) clays and peat are key issues for a proper management of settlement-affected urban areas. Indeed, ground settlements related to subsidence phenomena of either natural or anthropogenic origin, or complex combinations of both, cause recurrent damage to affected facilities (e.g., buildings) resulting in economic losses of billions of US Dollars per year (Bucx et al. 2015). The subsidence-related problems are often exacerbated by decay processes (due to fungal or bacteria attack) affecting wooden piles (Klaassen and Creemers 2012). For this reason, both scientists and technicians as well as civilian communities are interested in studies aimed at analyzing and predicting the consequences to buildings in subsiding areas in order to select the most suitable strategies for

F. Calvetti et al. (Eds.): CNRIG 2019, LNCE 40, pp. 42–51, 2020.
https://doi.org/10.1007/978-3-030-21359-6_5

land-use planning and urban management purposes. In this regard, the use of probabilistic approaches oriented to the generation of empirical fragility (Peduto et al. 2017b, 2019) and vulnerability curves (Peduto et al. 2018) are particularly promising, provided that a comprehensive dataset on both subsidence-related intensity (SRI) parameters and corresponding damage severity to buildings is available.

In this paper a rich sample of more than seven hundred monitored and surveyed masonry buildings – mainly resting with their (shallow or wooden pile) foundations on soft soils – is analyzed in four urban areas in The Netherlands. Both deterministic empirical cause–effect relationships and probabilistic functions in the form of empirical fragility curves are retrieved for masonry buildings considering three different SRI parameters (i.e., differential settlement, rotation and deflection ratio) – derived from the processing of satellite Synthetic Aperture Radar (SAR) images by way of an interferometric (PSI) technique – in combination with severity levels of damage recorded from visual inspections on masonry buildings. Moreover, referring to the most suitable SRI parameter (among those selected) to be used for building settlement-induced damage analysis, an empirical vulnerability curve is generated for masonry buildings with wooden pile foundations.

2 The Proposed Methodology

The methodological approach for the vulnerability analysis of settlement-affected masonry buildings with shallow/piled foundations in soft soils is shown in Fig. 1.

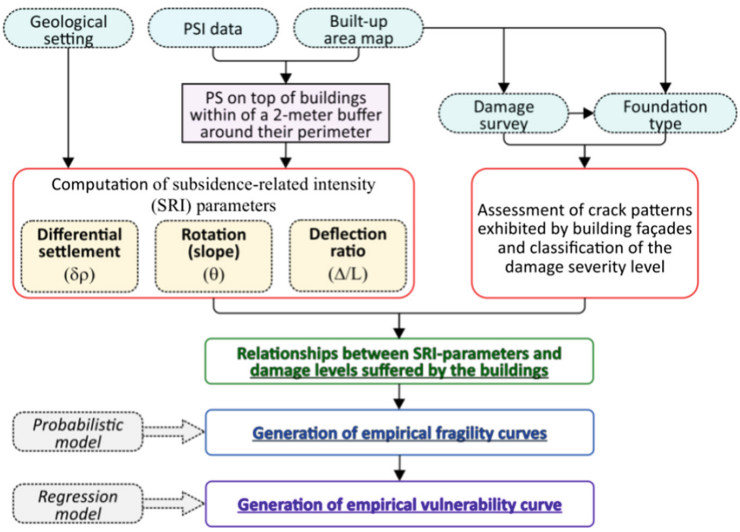

Fig. 1. Flowchart of the proposed methodology.

Following cascading steps, both empirical fragility and vulnerability curves are generated starting from a set of input data including: *(i)* geo-lithological properties of

the involved soils; *(ii)* PSI-derived displacement measurements; *(iii)* built-up area map; *(iv)* information gathered from the visual inspection of crack patterns experienced by building façades via in-situ damage surveys and *(v)* building foundation type. In particular, first PSI-data are filtered based on their elevation and the built-up area map so as to select PSs on top of the buildings falling within a 2-meter buffer around the building's perimeter. These data are used to compute different SRI parameters of foundation movements affecting a sample of masonry buildings in similar geo-lithological settings (i.e., presence of soft soil strata). In particular, three SRI parameters are taken into account: *(i)* the differential settlement ($\delta\rho$), computed along a given PS-derived settlement profile as the difference between maximum and minimum recorded settlements values; *(ii)* the rotation (θ), or slope, assumed as $\theta = \delta\rho/L\rho$, where $L\rho$ indicates the distance at the foundation level between the two points where $\delta\rho$ was computed and *(iii)* the deflection ratio (Δ/L), derived according to the definition provided by Burland and Wroth (1974), as the ratio between the displacement (Δ) of a point relative to the line connecting two consecutive inflection points and the distance L between two consecutive points of inflection. Moreover, for each analyzed building, the deflection ratio is computed for both sagging and hogging zones (if any) and the highest obtained value is associated with the corresponding building damage severity level. The latter, derives from the analysis of crack patterns experienced by the building façades using the information collected during in-situ damage surveys via ad-hoc predisposed building fact-sheets (Peduto et al. 2017b) and classified adapting the ranking proposed by Burland et al. (1977).

The information collected on buildings, homogenized based on their foundation type (e.g., shallow or wooden pile foundations), preliminarily allows retrieving the relationships between the selected SRI parameters and the damage severity levels; then, it is used for the generation of empirical fragility curves by adopting a probabilistic model. To this aim, the probability $P(\cdot)$ for a randomly selected building to reach, or exceed, a certain damage severity level (Di) for a given value of the selected SRI parameter, is assessed as (Shinozuka et al. 2000; Peduto et al. 2017b, 2019):

$$P(Damage \geq Di|SRI_i) = \Phi\left[\frac{1}{\beta_i} ln\left(\frac{SRI}{\overline{SRI}_i}\right)\right] \quad (1)$$

In the Eq. 1 the fragility parameters (median $\overline{SRI}_i$ and standard deviation β_i) of the used standard normal cumulative distribution function $\Phi[\_]$ are computed using the maximum likelihood estimation method (Shinozuka et al. 2003). Finally, the empirical vulnerability curve relating the most suitable SRI parameter (among those selected) to be used for building settlement-induced damage analysis with the expected mean level of damage severity (μ_D) is derived by fitting the $\mu_D(SRI_i)$ data obtained as (adapted from Pitilakis and Fotopoulou 2015):

$$\mu_D(SRI_i) = \sum_{i=0}^{1} P_i * d_i \quad (2)$$

where P_i is the discrete probability associated with a damage severity level (Di) whose numerical index equals d_i, using as regression model the tangent hyperbolic function (Lagomarsino and Giovinazzi 2006; Peduto et al. 2017a):

$$\mu_D = a[b + \tanh(c * SRI_i + d)] \tag{3}$$

where a, b, c, and d are four fitting coefficients that must be determined for the building sample.

3 Case Studies and Available Dataset

The case studies selected for the analysis are four urban areas in The Netherlands: Schiedam, Rotterdam, Dordrecht and Zaanstad (Fig. 2). They suffer from widespread ground settlements mainly associated with the presence of highly compressible fine-grained "soft soils", e.g. clay and peat in the upper strata (Den Haan and Kruse 2006). Moreover, in these areas decay processes (due to fungal or bacteria attack) widely affect wooden piles (Klaassen and Creemers 2012) often compromising their functionality. The geo-lithological setting of the involved soils, including the probability of occurrence of each lithological class, was gathered from the nationwide 3D geological 'GeoTOP' model built by the Geological Survey of The Netherlands via the collection and analysis of hundreds of thousands of borehole data and cone penetration tests (Stafleu et al. 2011). The model provides information on the lithology of the Dutch subsoil on millions of voxels - each measuring l00 × l00 × 0.5 m (height × width × depth) - down to a depth of 50 m below the ground surface. Figures 2a (Schiedam), c (Rotterdam), e (Dordrecht), g (Zaanstad) show the cumulative thicknesses of soft soils in the study areas jointly with the typical Dutch geological setting – consisting of Holocene clayey and peaty layers alternating with lenses of sandy soils and superimposed to sandy deposits of Pleistocene age – extracted from generic cross-sections sketched along the A-A' profiles. As for PSI data used for the analyses, with reference to all the municipalities, high-resolution images acquired by TerraSAR-X (TSX) radar sensor on both ascending and descending orbits in the period spanning from 2009 to 2015 – processed via the commercial chain 'Antares' based on the PSI algorithm (Ferretti et al. 2001) – are available. Since subsidence-related displacements are assumed as mainly vertical, the recorded PSI-velocities were projected from the line of sight sensor-target direction (LOS) to the vertical direction (Nicodemo et al. 2017; Peduto et al. 2017b, 2019) whose spatial distribution is shown, for the four investigated municipalities, in the Figs. 2b, d, f and h, respectively. The sample of analyzed buildings consists of 706 low-rise masonry buildings (2–3 floors), whose age dates back to the beginning of the 19th century up to about the 1980s, mainly of brick and lime mortar with either shallow or (wooden) piled foundations. On these buildings, an extensive damage survey was carried out in April 2015 and July 2016 (Peduto et al. 2019) that allowed investigating – through the analysis of crack patterns – both the distribution and the severity of damage suffered by the buildings, whose levels are classified in six classes (D0 = no damage; D1 = very slight; D2 = slight; D3 = moderate; D4 = severe; D5 = very severe) adapting those provided by Burland et al. (1977). The results of the buildings survey campaign are summarized in Table 1.

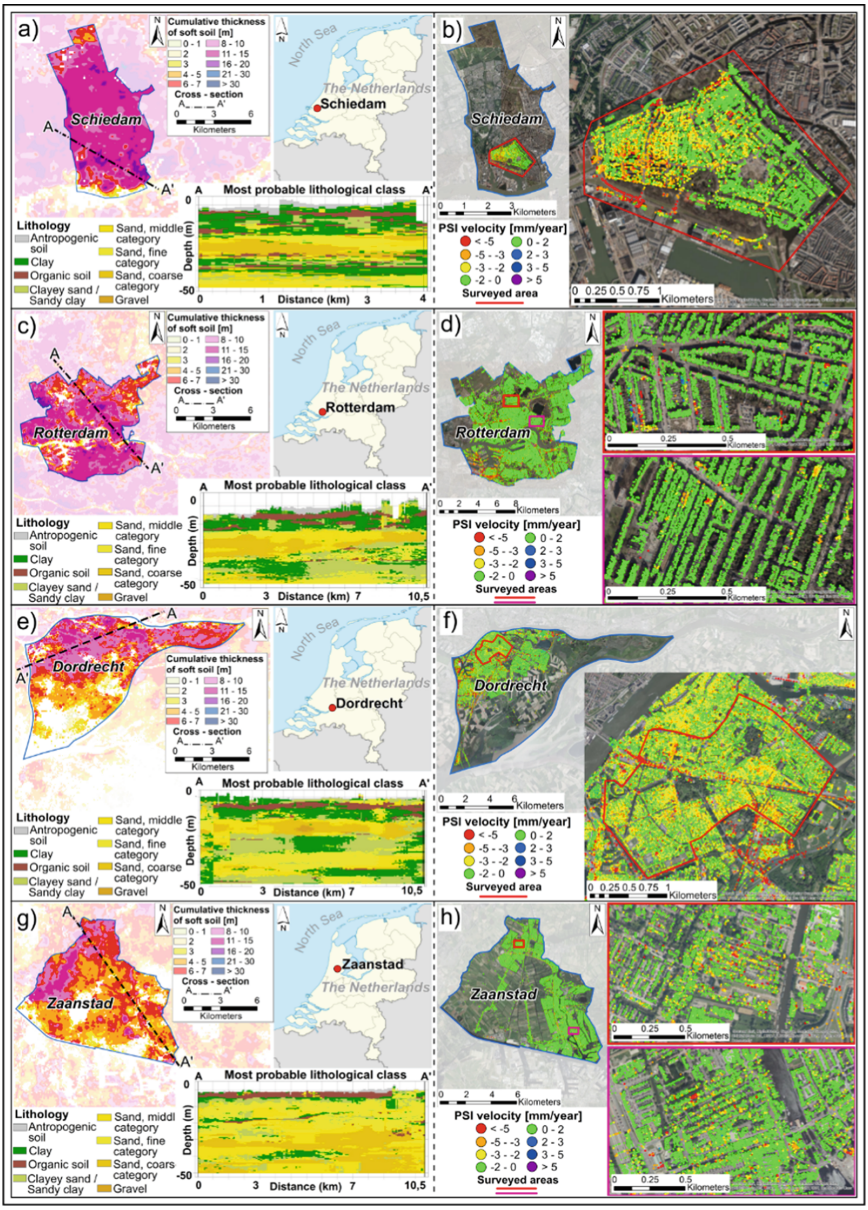

Fig. 2. Analyzed study areas and available PSI dataset: cumulative thickness of soft soils (organic and clayey) and geological cross-section along the A–A' profile sketch for (a) Schiedam, (c) Rotterdam, (e) Dordrecht and (g) Zaanstad municipalities; PSI data on ascending and descending orbit on top of the buildings provided by the TSX radar sensor for (b) Schiedam, (d) Rotterdam, (f) Dordrecht and (h) Zaanstad municipalities (modified from Peduto et al. 2019).

Table 1. Number of surveyed masonry buildings for each analyzed study area distinguished according to the foundation type and recorded damage severity levels.

Study area	Foundation type	Number of buildings						
		Damage level						TOT.
		D0	D1	D2	D3	D4	D5	
SCHIEDAM	Shallow	53	21	24	6	0	0	104
	Piled	112	56	33	5	0	0	206
ROTTERDAM	Shallow	0	0	0	0	0	0	0
	Piled	102	43	18	11	9	0	183
DORDRECHT	Shallow	56	9	5	6	0	0	76
	Piled	23	16	9	4	2	2	56
ZAANSTAD	Shallow	0	0	0	0	0	0	0
	Piled	8	31	20	16	6	0	81

4 Results

According to the methodology described in Sect. 2, three SRI parameters (δρ, θ and Δ/L) were computed for each analyzed building. To this aim, the vertical PSI-derived settlement measurements were interpolated within the building's perimeter (Fig. 3a) (Nicodemo et al. 2017; Peduto et al. 2017b) and the intensity SRI parameters were assessed along a longitudinal cross-section of the building (Fig. 3b).

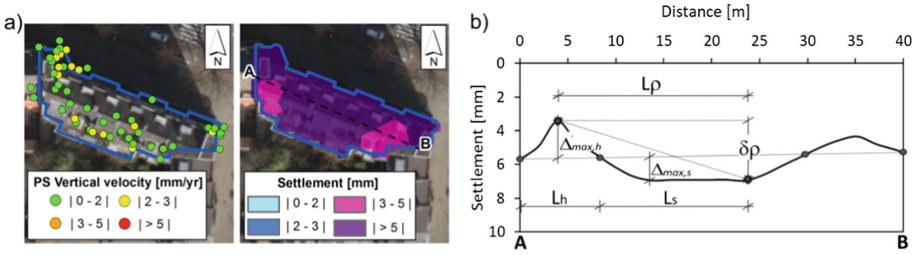

Fig. 3. Sketch synthesizing the computation of the PSI-derived SRI parameters: (a) map of PS vertical velocity and cumulative settlement; (b) selected SRI parameters (differential settlement δρ, rotation θ and deflection ratio Δ/L).

Considering the similar subsoil settings/properties (i.e., the presence of soft soil layers) as well as foundation and structural typology, the results of the four investigated areas first were combined into one dataset. Then, cause-effect relationships between the magnitude of the selected SRI parameters and damage severity levels were derived for the analyzed buildings grouped according to their shallow (Figs. 4a, c and e) or wooden pile foundations (Figs. 4b, d and f). In this phase, a unique damage class (D4/D5) was considered for the buildings with damage level classified as D4 and D5 due to the limited number of buildings falling in these classes. The plotted graphs

(Fig. 4) show, for both foundation types (shallow and wooden pile), a generally increasing trend of the damage severity level for higher values of the considered SRI intensity parameters.

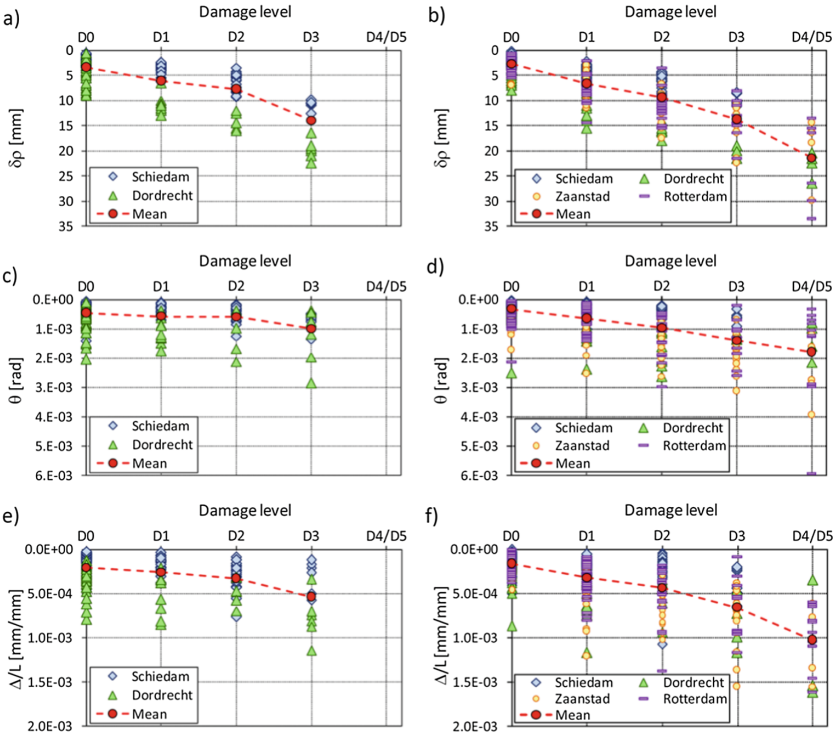

Fig. 4. Damage level vs. SRI parameters for surveyed building in the study areas with (a), (c), (e) shallow and (b), (d), (f) piled foundations (modified from Peduto et al. 2019).

Then, starting from the diagrams of Fig. 4, empirical fragility curves were generated using the Eq. 1 for both building samples with shallow (Figs. 5a, c and e) and piled (Figs. 5b, d and f) foundations. The values of corresponding fragility parameter are summarized in Table 2.

The obtained cause-effect relationships (Fig. 4) and the derived empirical fragility curves (Fig. 5) highlight that δρ is the SRI parameter that works best since its arithmetic mean values (Figs. 4a and b) can be more easily associated with distinct damage severity levels. Furthermore, the fragility curve obtained for θ and Δ/L (Fig. 5) tends to be convex upward in shape (i.e. the existence of an inflection point cannot be clearly recognized), with probability of reaching or exceeding a given damage severity level for unrealistic values of the considered SRI parameter with respect to limiting values proposed in the literature (e.g., Skempton and MacDonald 1956).

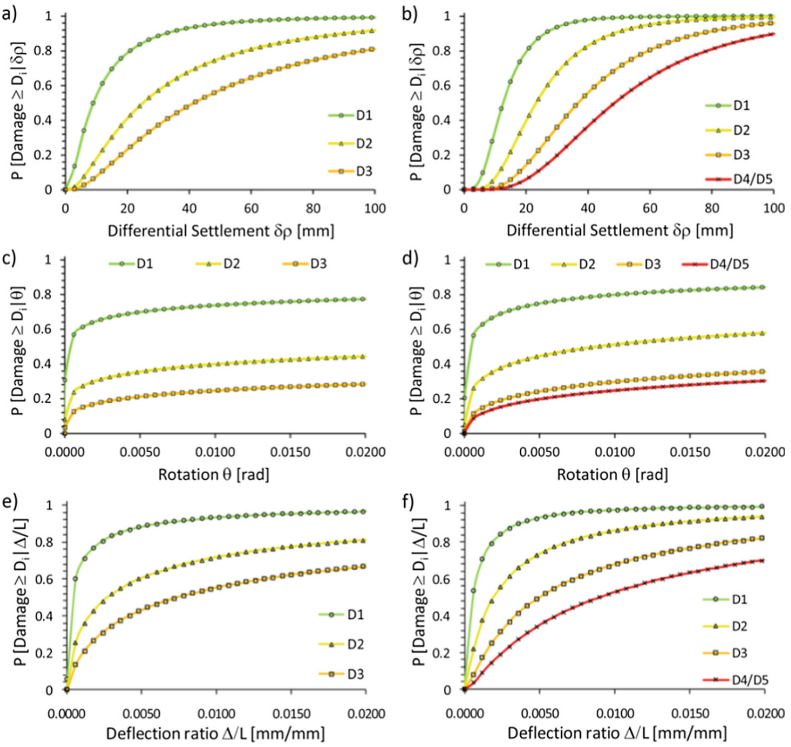

Fig. 5. Fragility curves for masonry building in the study areas with (a), (c), (e) shallow and (b), (d), (f) piled foundations distinguished according to considered SRI parameters (modified from Peduto et al. 2019).

Table 2. Fragility parameters (median, $\overline{SRI_i}$ and standard deviation, β) for each considered intensity (SRI) parameter distinguished according to the foundation type and damage severity levels.

SRI parameter	Damage level	Foundation type			
		Shallow		Piled	
		$\overline{SRI_i}$	β_i	$\overline{SRI_i}$	β_i
δρ [mm]	D1	9.04	0.99	12.57	0.57
	D2	25.06	0.99	23.26	0.57
	D3	41.53	0.99	36.81	0.57
	D4/D5	-	-	48.60	0.57
θ [rad]	D1	2.16×10^{-4}	6.04	3.10×10^{-4}	4.14
	D2	4.67×10^{-2}	6.04	8.69×10^{-3}	4.14
	D3	6.38×10^{-1}	6.04	9.08×10^{-2}	4.14
	D4/D5	-	-	1.69×10^{-1}	4.14
Δ/L [mm/mm]	D1	3.46×10^{-4}	2.25	5.32×10^{-4}	1.50
	D2	2.74×10^{-3}	2.25	1.95×10^{-3}	1.50
	D3	7.45×10^{-3}	2.25	5.01×10^{-3}	1.50
	D4/D5	-	-	9.00×10^{-3}	1.50

Finally, assuming δρ as the most suitable SRI parameter (among the selected ones) for building settlement-induced damage analysis, an empirical vulnerability curve (Fig. 6) was generated for masonry buildings with piled foundation (whose damage severity levels span from D1 to D5), by fitting the μ_D data (obtained from Eq. 2 considering for this application a numerical index *di* equal to 0.25, 0.50, 0.75, and 1 for D1, D2, D3, and D4/D5, respectively) through the Eq. 3; the fitting coefficients equalled: a = 0.586, b = 0.705, c = 0.041, and d = − 0.968.

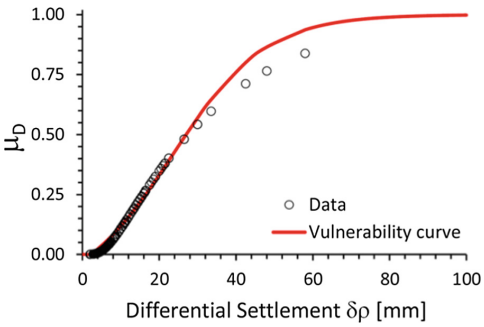

Fig. 6. Vulnerability curve for masonry building with piled foundations in term of the differential settlement (δρ) as the representative SRI parameter.

5 Conclusions

In this paper, the results of an extensive in-situ campaign of visual inspections of more than 700 masonry buildings located in four municipalities in The Netherlands were combined with different PSI-derived SRI (differential settlement δρ, rotation θ and deflection ratio Δ/L) parameters to retrieve *(i)* empirical relationships between the recorded damage severity levels and the intensity of the selected SRI parameter, *(ii)* empirical fragility curves for masonry buildings with different foundation types (either shallow or wooden piled), *(iii)* the identification of δρ as the most suitable SRI parameter (among those selected) to be used for building settlement-induced damage analysis. This latter, was used to generate an empirical vulnerability curve for masonry buildings with wooden pile foundation.

The presented study deserves further deepening concerning the role of predisposing factors to building settlements in the study area such as, for instance, presence/thickness of soft soil layers and lowering (though rather limited in The Netherlands) of the groundwater table.

However, considering the encouraging outcomes, these predictive tools – once further validated – could be valuably used within procedures aimed at investigating the building vulnerability in subsidence-affected urban areas and exported for forecasting purposes in all municipalities presenting similar geo-lithological and soils characteristics as well as urban fabric and foundation types.

References

Bucx THM, van Ruiten G, Erkens G, de Lange G (2015). An integrated assessment framework for land subsidence in delta cities. In: Proceedings IAHS, 372, prevention and mitigation of natural and anthropogenic hazards due to land subsidence, Copernicus Publication, pp 485–491

Burland JB, Broms BB, de Mello VFB (1977) Behaviour of foundations and structures. In: SOA report, proceedings of the 9th international conference on soil mechanics and foundation engineering, vol 2. Tokyo, pp 495–546

Burland JB, Wroth CP (1974) Settlement of buildings and associated damage. In: SOA review. Proc. conference on settlement of structures, Cambridge, Pentech Press, London, pp 611–654

Den Haan EJ, Kruse GAM (2006) Characterisation and engineering properties of Dutch peats. In: Tan et al. (eds) Characterization and engineering properties of natural soils 3, Taylor & Francis Group, London, pp 2101–2133

Ferretti A, Prati C, Rocca F (2001) Permanent scatterers in SAR interferometry. IEEE Trans Geosci Remote Sens 39(1):8–20

Klaassen RKWM, Creemers JGM (2012) Wooden foundation piles and its underestimated relevance for cultural heritage. J Cult Heritage 13:123–128

Lagomarsino S, Giovinazzi S (2006) Macroseismic and mechanical models for the vulnerability and damage assessment of current buildings. Bull Earthq Eng 4(4):415–443

Nicodemo G, Peduto D, Ferlisi S, Maccabiani J (2017) Investigating building settlements via very high resolution SAR sensors. In: Life-cycle of engineering systems: emphasis on sustainable civil infrastructure, Taylor & Francis Group, London, pp 2256–2263

Peduto D, Ferlisi S, Nicodemo G, Reale D, Pisciotta G, Gullà G (2017a) Empirical fragility and vulnerability curves for buildings exposed to slow-moving landslides at medium and large scales. Landslides 14(6):1993–2007

Peduto D, Korff M, Nicodemo G, Marchese A, Ferlisi S (2019) Empirical fragility curves for settlement-affected buildings: analysis of different intensity parameters for seven hundred masonry buildings in The Netherlands. In press on *Soils Found*. https://doi.org/10.1016/j.sandf.2018.12.009

Peduto D, Nicodemo G, Maccabiani J, Ferlisi S (2017b) Multi-scale analysis of settlement induced building damage using damage surveys and DInSAR data: A case study in The Netherlands. Eng Geol 218:117–133

Peduto D, Nicodemo G, Caraffa M, Gullà G (2018) Quantitative analysis of consequences induced by slow-moving landslides to masonry buildings: a case study. Landslides 15 (10):2017–2030

Pitilakis KD, Fotopoulou SD (2015) Vulnerability assessment of buildings exposed to coseismic permanent slope displacements. In: Winter et al. (eds) Geotechnical engineering for infrastructure and development, ICE Publishing, pp 151–173

Shinozuka M, Feng MQ, Kim HK, Uzawa T, Ueda T (2003) Statistical analysis of fragility curves. *Technical report MCEER-03-0002*, State University of New York, Buffalo

Shinozuka M, Feng Q, Lee J, Naganuma T (2000) Statistical analysis of fragility curves. J Eng Mech 126(12):1224–1231

Skempton AW, MacDonald DH (1956) Allowable settlement of buildings. In: Proceedings of the ICE (Institute of Civil Engineers), Pt. III, Vol 5, pp 727–768

Stafleu J, Maljers D, Gunnink JL, Menkovic A, Busschers FS (2011) 3D modeling of the shallow subsurface of Zeeland, The Netherlands. Netherlands Journal of Geosciences-Geologie En Mijnbouw 90(4):293–310